

A MEASUREMENT OF $\alpha_s(Q^2)$ FROM THE GROSS-LLEWELLYN SMITH SUM RULE

J. H. Kim², D. A. Harris⁶, C. G. Arroyo², L. de Barbaro⁵, P. de Barbaro⁶, A. O. Bazarko², R. H. Bernstein³, A. Bodek⁶, T. Bolton⁴, H. Budd⁶, J. Conrad², R. A. Johnson¹, B. J. King², T. Kinnel⁷, M. J. Lamm³, W. C. Lefmann², W. Marsh³, K. S. McFarland³, C. McNulty², S. R. Mishra², D. Naples⁴, P. Z. Quintas², A. Romosan², W. K. Sakumoto⁶, H. Schellman⁵, F. J. Sciulli², W. G. Seligman², M. H. Shaevitz², W. H. Smith⁷, P. Spentzouris², E. G. Stern², M. Vakili¹, U. K. Yang⁶, J. Yu³

(1) *University of Cincinnati, Cincinnati, OH 45221 USA*;

(2) *Columbia University, New York, NY 10027 USA*;

(3) *Fermi National Accelerator Laboratory, Batavia, IL 60510 USA*;

(4) *Kansas State University, Manhattan, KS 66506 USA*;

(5) *Northwestern University, Evanston, IL 60208 USA*;

(6) *University of Rochester, Rochester, NY 14627 USA*;

(7) *University of Wisconsin, Madison, WI 53706 USA*

(February 13, 2018)

We extract a set of values for the Gross-Llewellyn Smith sum rule at different values of 4-momentum transfer squared (Q^2), by combining revised CCFR neutrino data with data from other neutrino deep-inelastic scattering experiments for $1 < Q^2 < 15 \text{ GeV}^2/c^2$. A comparison with the order α_s^3 theoretical predictions yields a determination of α_s at the scale of the Z-boson mass of $0.114 \pm .009$. This measurement provides a new and useful test of perturbative QCD at low Q^2 , because of the low uncertainties in the higher order calculations.

PAC Numbers: 12.38.Qk 11.55.Hx 13.15.+g 24.85.+p

The Gross-Llewellyn Smith (GLS) sum rule [1] predicts the integral $\int_0^1 (xF_3) \frac{dx}{x}$, where $xF_3(x, Q^2)$ is the non-singlet structure function measured in neutrino-nucleon (νN) scattering. In the naive quark parton model, the value of this integral should be three, the number of valence quarks in the nucleon. In perturbative Quantum Chromodynamics (pQCD), this integral is a function of $\alpha_s(Q^2)$, the strong coupling constant.

The GLS integral is one of the few physical quantities which has been calculated to next-to-next-to-leading-order (NNLO) of perturbative QCD [2], and there are estimates of the next order term [3] (i.e. $O(\alpha_s^4)$). In addition, there is a non-perturbative higher-twist contribution, proportional to $1/Q^2$. This yields the GLS integral as a function of α_s , of the form:

$$GLS = 3 \left[1 - \frac{\alpha_s}{\pi} - a(n_f) \left(\frac{\alpha_s}{\pi} \right)^2 - b(n_f) \left(\frac{\alpha_s}{\pi} \right)^3 \right] - \frac{\Delta HT}{Q^2} \quad (1)$$

where $a(n_f)$ and $b(n_f)$ are functions [2] of the number of quark flavors accessible at a given Q^2 . The higher-twist correction term ΔHT is predicted to be significant in some models [4], while others [5–7] predict a negligibly small correction term. We take ΔHT as half the largest model prediction, with errors which cover the full range

$(\Delta HT = 0.15 \pm .15 \text{ GeV}^2)$.

The size and Q^2 -variation of the GLS integral is a robust prediction in pQCD. The NNLO calculation has been shown to be largely independent of renormalization scheme [8], and xF_3 is inherently independent of the gluon distribution. The number of orders to which the integral has been calculated ensures an accurate perturbative calculation in spite of the large value of α_s at low Q^2 .

An earlier measurement of the GLS integral has been published by the CCFR collaboration [9]. That analysis used a leading-order(LO) QCD-based fit to extrapolate all data to $Q^2 = 3 \text{ GeV}^2$, fitted the extrapolated data to a single function over all x , and numerically integrated that function. This was confirmed by a LO global fit analysis of the same data [10]. However, these approaches cannot make full use of the accuracy of the NNLO calculation shown above, since they depend on LO pQCD for extrapolation. Also, the previous CCFR analysis did not correct for quark mass thresholds [8], target mass [11] or higher-twist [4–7] effects. These corrections are important at the effective mean Q^2 of the result ($Q^2 \sim 3 \text{ GeV}^2$).

This paper describes a new GLS analysis, which uses revised CCFR xF_3 data together with data from earlier neutrino-scattering experiments. By combining data sets, we expand the kinematic region to measure $\int xF_3 \frac{dx}{x}$ for $1 < Q^2 < 15 \text{ GeV}^2$ without any extrapolation in Q^2 . This technique thus allows us to consistently use the fundamental NNLO prediction shown in equation (1).

The CCFR data were collected at Fermilab in experiments E744 and E770, which ran in 1985 and 1987-8 respectively. The experiments observed neutrino scattering in an iron calorimeter [12]. The calorimeter and muon spectrometer were calibrated using a test beam [13]. New structure functions (SFs) from this data [14] were published in 1997. These SFs had a number of improvements compared to the SFs used in the previous GLS measurement [9]. Improvements include a revised energy cali-

bration based directly on test-beam data, an improved calculation of radiative corrections [15], and the removal of and correction for two-muon events ($\nu N \rightarrow \mu^+ \mu^- X$) from the data sample. Previously, the two-muon events introduced a small ambiguity at low x between neutrino-induced and anti-neutrino-induced events, which is particularly important to the GLS integral.

This analysis further improves the CCFR structure functions [14] at low x by improving the acceptance and smearing corrections. These corrections, which require a cross-section model, now incorporate measurements of the strange sea [16] and a more accurate parameterization of the parton distributions. These procedures create a new SF set [17] with reduced uncertainty at low x .

We also expand our kinematic region at high x by using xF_3 data from other ν -N experiments, namely: WA25 [18], WA59 [19], SKAT [20], FNAL-E180 [21], and BEBC-Gargamelle [22]. These were each normalized to CCFR in the regions of overlap, and the WA25 data were corrected at high x for nuclear differences [23] in the targets.

The GLS integral is evaluated numerically using the combined xF_3 data in bins of x and Q^2 . The integral over x is evaluated separately for each Q^2 bin. At very low x we must extrapolate below the CCFR kinematic limit, while at high x we use other experiments' data, and interpolate as necessary within the large bins. In each case, we vary the forms of the interpolations and extrapolations, and use the differences in the integral as estimates of the systematic uncertainties in the procedures.

The CCFR data have a minimum x of roughly ($x = 0.002 \times Q^2$). To extrapolate below this, we fit a power law (Ax^B) to all points with $x < 0.1$. The power-law form is suggested by Regge theory [24], which predicts a shape of $x^{0.5}$. To test this assumption, we made an alternate fit of the form $Cx^{0.5}$, using the difference as an independent systematic uncertainty. This systematic error becomes large at Q^2 above 5 GeV^2 .

For $x > 0.5$, there are also few data points. Most of the data here come from BEBC and SKAT which quote only two points for the range $0.5 < x < 1.0$. Here xF_3 is steeply falling and thus the precise shape is important for integration. Again, to estimate the contribution and error we use various assumptions. For the central value, we use the principle that at high x , the shape of xF_3 should be the same as F_2 , since the sea quarks are negligible at high x . Electron scattering experiments at SLAC have precisely measured F_2 in this region [25]. These data are corrected for nuclear effects [23] and differences between eN and νN scattering [14]. The corrected F_2 data by itself give the same result as interpolating the xF_3 data with the F_2 shape.

However, the SLAC data have small resonance peaks which may be different from neutrino resonances. To estimate the systematic error, we take the difference be-

tween two power-law fits to the xF_3 data, using the forms $D(1 - x)^E$ and $F(1 - x)^3$. These bracket the SLAC fit and serve as the limits of reasonable interpolation forms. Note that resonance behavior at low Q^2 coupled with approximate scaling [26] leads to a predicted form of $(1 - x)^3$.

Fig. 1 shows the combined xF_3 data on a log x scale in four low- Q^2 regions, along with a line representing the power law fit (Ax^B) for $x < 0.1$ and the χ^2 for the fits. Fig. 2 shows the same data on a linear x scale to highlight the high- x region.

Following the procedure of the BEBC collaboration [22], we add the quasi-elastic contribution and correct the GLS integral for target mass effects. This is necessary to be consistent with theoretical prediction of higher-twist contributions [4] to the GLS integral. Table I shows the exact Q^2 ranges of each bin and the contributions to $\int xF_3 \frac{dx}{x}$ for the different regions of x .

The systematic uncertainties are divided into three classes. The first includes calibration, normalization, and other purely experimental issues. The second is uncertainty in the integration of experimental xF_3 , estimated by varying the assumed functional forms as described above. The third class includes uncertainties in the theoretical prediction of the GLS integral itself. A summary of all the uncertainties is shown in Table II.

The dominant experimental systematic uncertainties are in the normalization of xF_3 , which comes from the total neutrino and anti-neutrino cross-sections (σ_ν and $\sigma_{\bar{\nu}}$). The absolute σ_ν is not measured by CCFR, so we use the world average [27,28] ($\sigma_\nu/E_\nu = 0.677 \pm .007 \times 10^{-38} cm^2/GeV$). The ratio $\sigma_{\bar{\nu}}/\sigma_\nu$ is measured by CCFR, and combined with the world average [28,29] yields $\sigma_{\bar{\nu}}/\sigma_\nu = 0.499 \pm .007$. Other experimental uncertainties include the energy scale calibration of the detector and the effects of charm production on the measured structure functions.

Additionally, there is a small uncertainty in the revised calculation of acceptance and smearing corrections. These corrections depend on a parameterization of the SFs. Variations of the functional form of the parameterization were used to estimate the systematic error.

The dominant theoretical uncertainty is the error on the higher-twist correction ($\Delta HT/Q^2$). Braun and Kolesnichenko [4] use three models which predict a correction term ΔHT between 0.16 and 0.29 GeV^2 . Other models, such as bag models [5] and a recent NNLO analysis [6] using a renormalon [7] approach, predict a negligible correction term ($\Delta HT < 0.02 GeV^2$). For our central value, we take $\Delta HT = 0.15 \pm .15 GeV^2$, thus covering all three predictions. The nuclear effects of the target are predicted to be small [30] ($-0.01/Q^2$ for iron). We also use estimates of the renormalization scheme dependence [8] and the order α_s^4 term in the pQCD expansion [3] as uncertainties in the perturbative calculation.

To extract a single value for $\Lambda_{\overline{MS}}^{(5)}$, we combine the measured values of the GLS integral in each Q^2 with the uncorrelated systematic errors, including the acceptance model error and the high- x and low- x fitting errors. These points are fitted to the NNLO pQCD function and higher-twist term, shown in Eq. (1). The prediction includes quark mass thresholds using the procedure of Chyla and Kataev [8]. The other systematic error sources are fully correlated in Q^2 , and are applied by shifting all GLS values by the uncertainty from that source and redoing the fit. The difference between the shifted and unshifted fit result represents the uncertainty in α_s from that systematic error.

The best fit to the measured GLS integral as a function of Q^2 is for a value of $\Lambda_{\overline{MS}}^{(5)} = 165 \text{ MeV}$. Evolving to M_Z^2 and 3 GeV^2 at NNLO, this corresponds to:

$$\alpha_s(M_Z^2) = 0.114 \pm .005 \text{ (stat)} \pm .007 \text{ (syst)} \pm .005 \text{ (thry)} \quad (2)$$

$$\alpha_s(3 \text{ GeV}^2) = 0.28 \pm .035 \text{ (stat)} \pm .05 \text{ (syst)} \pm .035 \text{ (thry)} \quad (3)$$

If the higher twist models of [5-7] are used, the central values become $\alpha_s(M_Z^2) = 0.118$ and $\alpha_s(3 \text{ GeV}^2) = 0.31$. Table III shows the results of fitting for $\Lambda_{\overline{MS}}^{(5)}$ at each Q^2 value as a consistency check. In all cases the small target mass and quasi-elastic corrections are included, and roughly cancel.

In conclusion, the GLS sum rule allows a precise measurement of α_s at low Q^2 . An independent measurement of α_s from the CCFR calculation [14] used the slope of global NLO fits to $x F_3$ and F_2 for $15 < Q^2 < 125 \text{ GeV}^2$, and found $\alpha_s(M_Z^2) = 0.119 \pm .004$. Three orders of magnitude higher in scale ($Q^2 = M_Z^2 = 8315 \text{ GeV}^2$), electroweak fits to LEP data [31] found $\alpha_s(M_Z^2) = 0.124 \pm .004 \pm .002$ based on the parameter R_ℓ .

The GLS result is consistent with other measurements, showing the power of pQCD across a very wide range of scales. An inconsistency in results might have indicated a need for higher order calculations in other measurements (i.e. NNLO) or the presence of other theoretical effects [32] which scale with Q^2 . The GLS result can be improved in the future by additional data from the NuTeV experiment at Fermilab and by better understanding of higher-twist effects.

ACKNOWLEDGMENTS

Acknowledgments. This research was supported by the U.S. Department of Energy and the National Science Foundation. We thank the staff of the Fermi National Accelerator Laboratory for their hard work in support of this experimental effort. We also wish to thank Andrei Kataev for helpful suggestions regarding the theoretical calculations.

- [1] D.J. Gross and C.H. Llewellyn Smith, Nucl. Phys. **B14**: 337 (1969).
- [2] S.A. Larin and J.A.M. Vermarseren, Phys. Lett. B259:1991345 Phys. Lett. **B259**: 345 (1991).
- [3] A.L. Kataev and V.V. Starshenko, Mod. Phys. Lett. **A10**: 235 (1995).
- [4] V.M. Braun and A.V. Kolesnichenko, Nucl. Phys. **B283**: 723 (1987).
- [5] S. Fajfer and R.J. Oakes, Phys. Lett. **B163**: 385 (1985).
- [6] A. Bodek and U.K. Yang, University of Rochester Preprint UR-1519 (1998)
- [7] M. Dasgupta and B. R. Webber, Phys. Lett. **B382**: 273 (1996).
- [8] J. Chyla and A.L. Kataev Phys. Lett. **B297**: 385 (1992).
- [9] W.C. Leung *et al.*, Phys. Lett. **B317**: 655 (1993).
- [10] A.L. Kataev, A.V. Sidorov *et al.*, Phys. Lett. **B331**: 179 (1994).
- [11] D.J. Gross *et al.*, Phys. Rev. **D15**: 2486 (1977).
- [12] W.S. Sakumoto *et al.*, Nucl. Instr. Meth. **A294**: 179 (1990).
- [13] B.J. King *et al.*, Nucl. Instr. Meth. **A302**: 254 (1991).
- [14] W.G. Seligman *et al.*, Phys. Rev. Lett. **79**: 1213 (1997).
- [15] D.Y. Bardin and O.M. Fedorenko, Sov. J. Nucl. Phys. **30(3)**: 418 (1979).
- [16] S.A. Rabinowitz *et al.*, Phys. Rev. Lett. **70**: 134 (1993).
- [17] Complete tables of the GLS revised SF results can be obtained from the World Wide Web via the URL <http://www-e815.fnal.gov/~jhkim/ccfrsf.html> .
- [18] D. Allasia *et al.*, Z. Phys. **C28**: 321 (1985).
- [19] K. Varvell *et al.*, Z. Phys. **C36**: 1 (1987).
- [20] V.V. Ammosov *et al.*, Z. Phys. **C30**: 175 (1986).
- [21] V.V. Ammosov *et al.*, JETP Lett. **36**: 367 (1982).
- [22] P.C. Bosetti *et al.*, Nucl. Phys. **B142**: 1 (1978).
- [23] D.F. Geesaman *et al.*, Ann. Rev. Nucl. Part. Sci. **45**: 337 (1995).
- [24] S.J. Brodsky and G. Farrar, Phys. Rev. Lett. **31**: 1153 (1973).
- [25] L.W. Whitlow *et al.*, Phys. Lett. **B282**: 475 (1992).
- [26] R.G. Roberts, *The Structure of the Proton*, p 37.
- [27] P.S. Auchincloss *et al.*, Z. Phys. **C48**: 411 (1990).
- [28] R. Blair *et al.*, Phys. Rev. Lett. **51**: 343 (1983). P. Berge *et al.*, Z. Phys. **C49**: 187 (1991).
- [29] W.G. Seligman, Nevis Report No. 292.
- [30] S.A. Kulagin, e-print archive: nucl-th/9801039.
- [31] D. Abbaneo *et al.*, CERN-PPE-97-154 (1997).
- [32] G.L. Kane, R.G. Stuart, J.D. Wells, Phys. Lett. **B354**: 350 (1995).

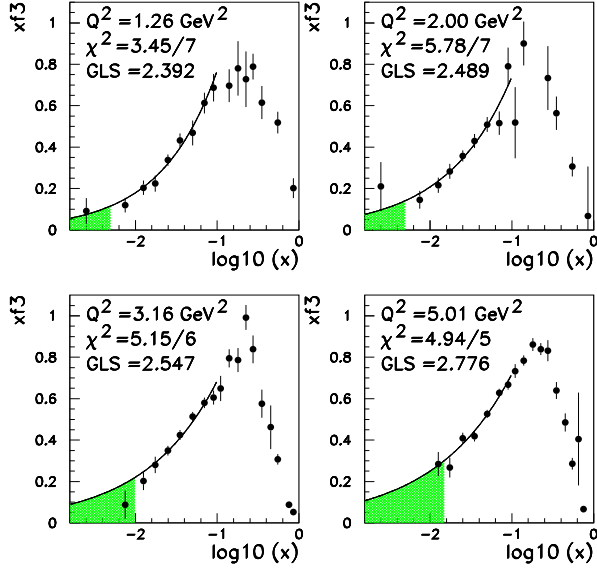


FIG. 1. xF_3 as a function of x at the four lowest Q^2 values, with x on a log scale. The area under the points thus represents $\int xF_3 \frac{dx}{x}$. The curve is a power law(Ax^B) fit to the $x < 0.1$ points, which is used to calculate the integral in the shaded region.

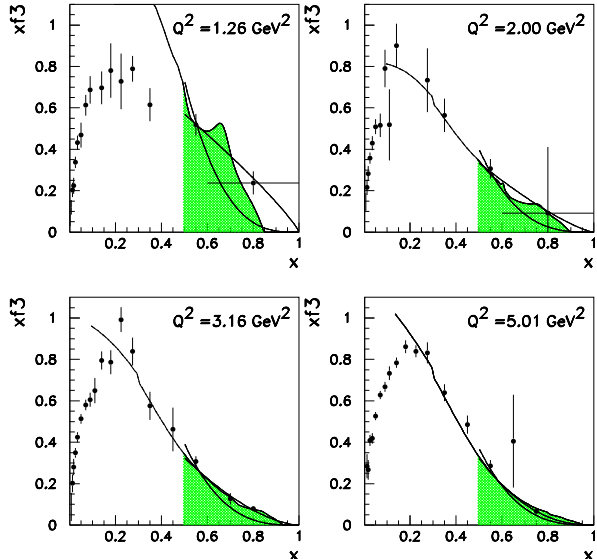


FIG. 2. xF_3 as a function of x at the four lowest Q^2 values, with x on a linear scale to show the high- x data. The shaded region shows the fit using the shape from SLAC F_2 data. The other lines are the power law fits ($D(1 - x)^E$ above and $F(1 - x)^3$ below) used to estimate systematic error.

TABLE I. The contributions to the GLS integral from different regions of x and the quasi-elastic peak added at $x = 1$, shown as a function of Q^2 (in GeV^2). For high and low x , it shows the estimated uncertainties due to the model choice only. The values include the target mass corrections.

Q^2	$\int_0^{.02} F_3 dx$	$\int_{.02}^{.5} F_3 dx$	$\int_{.5}^1 F_3 dx$	qElas
1.0- 1.6	$0.376 \pm .082$	1.730	$0.183 \pm .073$	0.103
1.6- 2.5	$0.523 \pm .002$	1.843	$0.091 \pm .026$	0.033
2.5- 4.0	$0.558 \pm .026$	1.889	$0.092 \pm .020$	0.009
4.0- 6.3	$0.700 \pm .137$	1.991	$0.084 \pm .016$	0.002
6.3-10.0	$0.748 \pm .139$	2.004	$0.064 \pm .008$	0.0004
10.0-15.5	$0.718 \pm .113$	2.007	$0.073 \pm .003$	0.0001

TABLE II. Uncertainties in $\alpha_s(M_Z^2)$. Errors which are uncorrelated in Q^2 are marked with a *. Other sources are fully correlated in Q^2 .

Source	Error
Statistical	$(+ .005)$ $(-.006)$
σ_ν Normalization	$(+ .003)$ $(-.005)$
$\sigma_\nu/\sigma_{\bar{\nu}}$ Ratio	$(+ .005)$ $(-.006)$
Energy Calibration	$(+ .002)$ $(-.003)$
Charm Production	$\pm .0005$
Acceptance model*	$\pm .002$
Total Experimental Error	$(+ .006)$ $(-.008)$
High- x fitting*	$\pm .003$
Low- x fitting*	$\pm .002$
Total Model Error	$\pm .004$
Combined Systematic Error	$(+ .007)$ $(-.009)$
Higher-twist	$(+ .004)$ $(-.005)$
Renormalization Scheme [8]	$\pm .001$
Order α_s^4	$\pm .0003$
Total Theory Error	$\pm .005$

TABLE III. The total GLS integral and α_s for each bin in Q^2 . The errors on the GLS are $\pm (stat) \pm (syst)$. The errors on $\alpha_s(Q^2)$ are $\pm (stat) \pm (syst) \pm (thry)$. Systematic errors are correlated in Q^2 .

$\langle Q^2 \rangle$	$GLS(Q^2)$	$\alpha_s(Q^2)$
1.26	$2.39 \pm .08 \pm .14$	$0.330 \pm .023 \pm .042 \pm .050$
2.00	$2.49 \pm .08 \pm .10$	$0.303 \pm .020 \pm .026 \pm .036$
3.16	$2.55 \pm .06 \pm .10$	$0.287 \pm .008 \pm .034 \pm .026$
5.01	$2.78 \pm .06 \pm .19$	$0.165 \pm .033 \pm .144 \pm .024$
7.94	$2.82 \pm .07 \pm .19$	$0.145 \pm .061 \pm .136 \pm .022$
12.59	$2.80 \pm .13 \pm .18$	$0.164 \pm .068 \pm .101 \pm .014$